Alda-1 restores ALDH2-mediated alcohol metabolism to inhibit the NF-κB/VEGFC axis in head and neck cancer

YU-HSUAN LIN[1-4], YI-CHEN LEE[5], JIA-BIN LIAO[6], PEI-LUN YU[7], CHIH-YU CHOU[7] and YI-FANG YANG[7]

[1]Department of Otolaryngology, Head and Neck Surgery, Kaohsiung Veterans General Hospital, Kaohsiung 813414, Taiwan, R.O.C.; [2]School of Medicine, National Yang Ming Chiao Tung University, Taipei 112304, Taiwan, R.O.C.; [3]School of Medicine, Chung Shan Medical University, Taichung 40201, Taiwan, R.O.C.; [4]School of Medicine, College of Medicine, National Sun Yat-sen University, Kaohsiung 804201, Taiwan, R.O.C.; [5]Department of Anatomy, School of Medicine, College of Medicine, Kaohsiung Medical University, Kaohsiung 807378, Taiwan, R.O.C.; [6]Department of Pathology and Laboratory Medicine, Kaohsiung Veterans General Hospital, Kaohsiung 813414, Taiwan, R.O.C.; [7]Department of Medical Education and Research, Kaohsiung Veterans General Hospital, Kaohsiung 813414, Taiwan, R.O.C.

Received August 30, 2024; Accepted December 12, 2024

DOI: 10.3892/ijmm.2025.5496

Abstract. The adaptation of cancer cells to hostile environments often necessitates metabolic pathway alterations to sustain proliferation and invasion. Head and neck cancer (HNC) has unfavorable outcomes. Therefore, elucidating the functional effects and molecular mechanisms underlying metabolic changes is key. Ingenuity Pathway Analysis identified 'ethanol degradation pathway II and IV' was consistently downregulated in tumor tissue, with aldehyde dehydrogenase 2 (*ALDH2*) emerging as a key prognostic gene among the top-ranked differentially expressed metabolic pathways. Immunohistochemistry (IHC) of HNC specimens revealed significant downregulation of ALDH2 expression in tumor tissue, which was inversely correlated with T classification, overall stage, recurrence rate and independently predicted poor prognosis. Functional assays showed that ALDH2 knockdown enhanced HNC cell migration, invasion and colony formation, while ALDH2 overexpression attenuated these processes. Mechanistically, ALDH2 downregulation and subsequent reactive oxygen species (ROS) production in cells activated NF-κB, upregulating vascular endothelial growth factor C (*VEGFC*) expression. ALDH2 overexpression inhibited ROS production and the NF-κB/VEGFC oncogenic pathway, with pharmacological inhibition of NF-κB and VEGFC mitigating the enhanced migration and invasion of ALDH2-knockdown HNC cells. IHC and transcriptome analysis further highlighted an inverse association between ALDH2 and VEGFC, with the $ALDH2^{high}/VEGFC^{low}$ profile predicting the most favorable survival outcome. Inhibition of ALDH2 with Daidzin increased *VEGFC* and phosphorylated NF-κB levels, restoring the migration and invasion of ALDH2-overexpressing HNC cells by enhancing the effects of VEGFC. Notably, modulating ALDH2 activity using Alda-1 ameliorated NF-kB/VEGFC axis upregulation following acetaldehyde treatment, aligning with the aforementioned alterations in alcohol metabolisms. These findings emphasize the key role of ALDH2 in influencing HNC progression and patient outcome, suggesting that targeting the ALDH2/NF-κB/VEGFC pathway may represent a potential therapeutic strategy for HNC.

Introduction

Head and neck cancer (HNC), the seventh most common type of cancer worldwide, poses a challenge to public health, with ~860,000 new cases and 450,000 deaths annually, as reported by GLOBOCAN 2020 (1). The key risk factors for HNC include tobacco and alcohol use, betel quid/areca nut consumption, human papillomavirus infection, and genetic alterations (2). Although certain HNC subgroups (such as human papillomavirus-associated HNC) (2) exhibit better survival prospects, the 5-year overall survival for HNC remains around 50%, even with comprehensive multi-disciplinary treatment (2,3). This situation underscores the need to identify novel therapeutic targets to enhance treatment efficacy and improve outcomes in patients with HNC.

Metabolic reprogramming, a hallmark of cancer, involves changes in energy metabolism and the reconfiguration of metabolic pathways. These adaptations, influenced by specific metabolites and enzymes, such as enhanced lactate as a consequence of aerobic glycolysis, create a tumor microenvironment conducive to tumor growth and progression (4,5). Despite the diverse and complex metabolic characteristics and preferences of tumors, marked alterations in metabolism are key for the initiation and progression of cancer (4,5). Therefore, identifying biomarkers with enzyme signatures reflecting

Correspondence to: Dr Yi-Fang Yang, Department of Medical Education and Research, Kaohsiung Veterans General Hospital, 386, Dajhong 1st Road, Zuoying, Kaohsiung 813414, Taiwan, R.O.C.
E-mail: yf@vghks.gov.tw

Key words: aldehyde dehydrogenase, NF-κB, VEGFC, head and neck cancer, alcohol metabolism pathway

altered metabolic pathways, particularly those associated with patient survival, is crucial. These biomarkers are essential for developing therapeutic strategies targeting tumor metabolism, offering a refined and potentially more effective approach to treating HNC.

Alcohol consumption increases the risk of numerous types of cancers, including HNC. The pathogenesis of alcohol-mediated cancer is influenced by various factors, notably aldehydic products such as acetaldehyde and 4-hydroxy-2-nonenal (4-HNE) (6,7). Acetaldehyde, the primary metabolite of ethanol, induces direct DNA damage by forming DNA adducts and compromises genomic stability by forming DNA-protein crosslinks and acetaldehyde-histone adducts (6-8). A previous study has highlighted the dose-dependent effect of alcohol consumption on the prognosis of patients with HNC, with this interplay influenced by aldehyde-detoxifying enzymes, such as ALDH2 (9). Given the poor prognosis of HNC and the pivotal role of metabolic reprogramming in cancer progression, this study aimed to investigate the links between metabolic pathway alterations and their contributions to tumorigenesis and cancer progression in patients with HNC, providing a foundation for potential therapeutic advancements.

Materials and methods

Metabolic pathway analysis. GSE6631 dataset, an mRNA microarray comparing 44 HNC with paired normal tissue controls, was downloaded from the Gene Expression Omnibus (GEO; ncbi.nlm.nih.gov/geo/). To identify genes with enzyme annotations that were significantly differentially expressed, fold-change was determined using GEO2R (ncbi.nlm.nih.gov/geo/info/geo2r.html#how_to_use). Ingenuity Pathway Analysis (IPA) was used to identify the metabolic pathways significantly altered in HNC tumor tissue (digitalinsights.qiagen.com/products-overview/discovery-insights-portfolio/analysis-and-visualization/qiagen-ipa/).

In silico mRNA profiles and Kaplan-Meier analysis. ENCORI database (starbase.sysu.edu.cn/index.php) was used to analyze the correlation between *ALDH2* and vascular endothelial growth factor C (*VEGFC*) mRNA expression. *VEGFC* mRNA levels in HNC tissue and its impact on overall survival of patients with varied *ALDH2* and *VEGFC* expression were investigated using the OncoLnc platform (oncolnc.org/). Gene expression analyses were conducted using GEPIA (gepia.cancer-pku.cn/), based on data from The Cancer Genome Atlas (TCGA) (10).

Clinical specimens and tissue microarrays for HNC. Tissue sample were fixed in 10% buffered formalin for 24 h at room temperature and embedded in paraffin. Paraffin-embedded sections of malignant tissue and their matched adjacent non-cancerous tissue (distance, >1 cm) were obtained from 106 patients diagnosed with HNC. The cohort included 91 male patients and 15 female pateints (age range: 27 to 87). Specimens were from patients without distant metastasis at the initial presentation, with histologically confirmed squamous cell carcinoma, and primary tumors located in the oral cavity, oropharynx, hypopharynx, or larynx. All the patients underwent surgical intervention at the Kaohsiung Veterans General Hospital, Kaohsiung, Taiwan between 2010/01 and 2016/12. Relevant clinical variables were recorded, including age, sex, American Joint Committee on Cancer (AJCC) T and N classification 11, overall stage (11), substance misuse, treatment strategy and disease status. Each discrete position within the initial tissue microarray (TMA-1) was configured to accommodate two cancer specimens and one adjacent non-cancerous specimen for quantification of protein levels. For additional analyses, a second microarray (TMA-2) was created from the same cohort. Due to sample loss during TMA-2 preparation, 84 samples were available. Ethics approval, including a waiver of informed consent, was granted by the Ethics Committee of Kaohsiung Veterans General Hospital (approval no. KSVGH23-CT8-10).

Immunohistochemistry. The 4-μm slides of the TMA paraffin block were used for IHC. TMA slides were deparaffinized in xylene, dehydrated using graded ethanols at room temperature. Briflyantigen retrieval from the TMA slides was performed using retrieval solution (Tris-EDTA buffer, pH 9.0) at 95˚C for 12 min and incuabated with peroxidase Blocking buffer (3% hydrogen peroxide) at room temperature for 10 min. Slides were incubated with blocking reagent (ready to use, BioTnA, TA00C2) for 30 min at room temperature. After blocking, slides were incubated with a primary antibody against ALDH2 (1:200; GTX101429, Genetex) and VEGFC (1:1,000, GTX113574, Genetex) for 1 h at room temperature. Expression level was determined by employing the HRP-conjugated secondary antibody (ready to use, TnAlink Polymer Detection System, cat. no. TACH02D, BioTnA,) for 30 min at room temperature, followed by 1 min of DAB (1:20) and 5 sec hematoxylin counterstaining at room temperature (TnAlink Polymer Detection System, TACH02D, BioTnA, Kaohsiung, Taiwan). The TMA slides were scanned by MoticEasyScan Pro (light microscope, 400x). A pathologist assessed the TMAs to exclude microarrays of suboptimal quality. Finally, quantification of ALDH2 and VEGFC IHC staining was performed using HistoQuest (TissueGnostics, version 7.1, Deep-learning nuclear segmentation program,). ALDH2 protein expression in cancer tissues was categorized into the high expression group, defined as >50% positive cells, and the low expression group (≤50% positive cells).

Cell culture. HNC cell lines SAS (Japanese Collection of Research Bioresources; cat. no. JCRB0260) and MTCQ1 (Bioresource Collection and Research Center, cat. no. 60620) were maintained in DMEM (HyClone; Cytiva; cat. no. SH30003.02) supplemented with 10% FBS (Cytiva, SH30396.03) and 1% penicillin-streptomycin-amphotericin (PSA; Biological Industries, 03-033-1B) at 37˚C in 5% CO_2. DOK (oral dysplasia), TW1.5 and TW2.6 (buccal mucosa) cell lines were maintained in DMEM/F12 (HyClone, SH30004.04) supplemented with 10% FBS and 1% PSA. DOK, TW1.5 (12,13) and TW2.6 were kindly provided by Dr Michael Hsiao (Academia Sinica, Taipei, Taiwan).

Lentivirus infection. Lentivirus vector control (pLKO-1-shLuc) and short hairpin (sh)ALDH2 viral supernatants (TRCN0000026452 and TRCN0000026486) were obtained from the National RNAi Core Facility (Taipei,

Taiwan). RNAi core based on 3rd Generation lentiviral guide, shRNA lentiviruses were produced by co-transfecting with hairpin-pLKO.1 vector (1 μg), VSV-G/pMDG2.G (0.1 μg), and pΔ8.91 (0.9 μg) constructs into 293T (American Type Culture Collection, CRL-3216™) cells using TransIT-LT1 transfection reagent (Mirus Bio, LLC; cat. no. #MIR 2300) and DNA complex incubated for 30 min at room temperature. After 40 h transfection, the viral supernatants were then harvested. Target sequences are listed in Table SI. Polybrene (8 μg/ml) was used to infect DOK or TW2.6 cells (1x10^5/well) using viral supernatants (5 multiplicity of infection). Following 72 h infection, cells were selected and maintained using 2 μg/ml puromycin (InvivoGen, ant-pr-5). Using 3rd Generation lentiviral guide, overexpression lentiviruses were produced by co-transfecting with cDNA-expressing vector (10 μg), pMDG (10 μg), and pΔ8.91 (1 μg) constructs into 293T cells using calcium phosphate (DNA complex incubated for 30 min at room temperature). After 48 h transfection, the viral supernatants were then harvested and concentrated by the Lentivirus Concentration kit (TopGen Biotechnology Co., Ltd., GM801-02). The lentiviral expression vector carrying human ALDH2 (NM_000690.4, pLVX-ALDH2-IRES-Neo) and control vector (pLVX-IRES-Neo) were acquired from TopGen Biotechnology Co., Ltd. Human ALDH2 cDNA was overexpressed in SAS and MTCQ1 cell lines. A total of 8 μg/ml polybrene was used to infect SAS or MTCQ1 cells (1x10^5/well) using viral supernatants (10MOI). After 72 h infection, the cells were selected and maintained using 400 μg/ml G418 Sulfate (Gibco™, 10131035). After 48 h selected and cultured for 48 h for subsequent analyses.

Reverse transcription-quantitative (RT-q)PCR. Total RNA was extracted from HNC cells using TRIzol® (Thermo Fisher Scientific, Inc.; cat. no. #15596018) following the manufacturer's instructions. cDNA was then synthesized using a PrimeScript™ RT Reagent kit (cat. no. #RR037A; Takara Biotechnology Co., Ltd.) according to the manufacturer's protocol. qPCR was performed using a SYBR Green PCR Master Mix (PCR Biosystems Ltd. qPCRBIO SyGreen Mix Lo-ROX) to evaluate target gene expression. Thermocycling conditions were as follows: Initial denaturation at 95˚C for 3 min; followed by 40 cycles of 95˚C for 10 sec and 60˚C for 30 sec. The $2^{-\Delta\Delta Cq}$ was used to calculate the results, and *ACTB* was used for normalization (14). The primers are listed in Table SII.

Gene expression evaluation using microarray analysis. Total RNA was isolated from TW2.6/shluc and TW2.6/shALDH2 cells using TRIzol® (Thermo Fisher Scientific, Inc.; cat. no. #15596018). Microarray analysis was performed on isolated RNA using a Clariom S Array, human (Applied Biosystems; Thermo Fisher Scientific, Inc.; cat. no. 902916) and scanned using an Affymetrix GeneChip Scanner 3000. To analyze the effects of *ALDH2* knockdown, an interaction network was generated using Qiagen GmbH IPA (QIAGEN 2000-2023) from TW2.6/shALDH2 cells, with the threshold set at 2-fold change. The microarray data were deposited in the GEO under accession no. GSE253622.

Boyden chamber assay. For invasion experiments, a polycarbonate membrane was pre-coated with fibronectin (10 μg, Thermo Fisher, 33016015) on the lower side and Matrigel (Corning, Inc.; cat. no. 354234) on the upper side at room temperature, 3 min. Migration assay used membranes without Matrigel pre-coating. The lower chamber was filled with complete culture medium (containing DMEM, 10% FBS). The cells (3x10^5/ml) were suspended in a serum-free DMEM, added to the 50 μl cells into upper chamber of each well and incubated at 37˚C in 5% CO_2 for 15-18 h. NF-κB inhibitor (Bay11-7082) was included in cells to perform the assay. To block VEGFC, we incubated TW2.6/shALDH2 cells with a VEGFC-neutralizing antibody (10-20 μg, GTX52393, GeneTex) for 30 min. After incubation, cells were trypsinized for migration and invasion assays, and a VEGFC-neutralizing antibody was added to the cells. After incubation, the cells were stained with crystal violet for 30 min at room temperature and counted under a light microscope (16x).

Cell viability assay. Cells (5,000 cells/well for DOK/shluc, DOK/shALDH2,TW2.6/shluc,TW2.6/shALDH2,SAS/Vector, and SAS/ALDH2) were plated in a 96 well plate with complete DMEM (10% FBS) mediaum for 24-72 h at 37˚C in 5% CO_2.

Using MTT (Sigma-Aldrich, 10 μl) for 4 h, the cell proliferation was assessed, and the signals were measured using an ELIAS reader (Thermo Fisher Scientific; Multiskan FC).

Immunoblotting. After extracting protein from the cell lines (DOK/shluc, DOK/shALDH2, TW2.6/shluc, TW2.6/shALDH2, SAS/Vector, and SAS/ALDH2) using RIPA lysis buffer [50 mM Tris-HCl, pH 8.0, 150 mM NaCl, 1% NP40, 1% sodium deoxycholate, 0.1% SDS, PMSF (0.1 mM), Na_3VO_4 (2 mM, and NaF (1 mM)] and protein concenteration were determined using Pierce™ BCA Protein Assay kits (ThermoFisher, 23225). Protein (50 μg) were loaded onto 10% SDS-PAGE for electrophoresis and subsequently transferred to a PVDF membrane and blocked with 5% non-fat dry milk in 1xPBST for 1 h at room temperature. The primary antibodies were incubated overnight at 4˚C. Table SIII lists the primary antibodies used for immunoblotting. The membranes were incubated with second antibodies [1:5,000, mouse (Jackson ImmunoResearch, 115-035-003), 1:5,000, rabbit (Jackson ImmunoResearch, 111-035-0031)] for 1 h at room temperature. The signals were visualised using an ECL™ Western Blotting Reagents (Cytiva, XR-IGE-RPN2106). ImageJ software (version 1.53t, National Institutes of Health) was used to quantify the densitometry.

Small interfering (si)RNA transfection. NF-κB p65 (RELA) siRNA, locus 11q13.1.; cat. no. #sc-29410 and control siRNA-A (cat. no. #sc-37007) were purchased from Santa Cruz Biotechnology, Inc. Next, 1x10^6 cells with complete media were plated in 6-cm plates for 24 h at 37˚C and subsequently transfected with 100 nM NF-κB p65 or control siRNA using TransIT-X2 (Mirus Bio, LLC; cat. no. #MIR 6000) and incubacted room temperature 30 min. Subsequent experiments were performed after 48 h.

Reactive oxygen species (ROS) quantification. Briefly, 2.5x10^4 cells/well were plated on a 96-well plate and incubated overnight at 37˚C in 5% CO_2. DCFDA (Abcam; cat. no. ab113851) was added to the cells and incubated at 37˚C

in 5% CO_2 for 45 min. After removing the DCFDA, cells were examined using a fluorescence plate reader (FLUOstar Omega; BMG Labtech GmbH).

Reporter assay. TW2.6/shluc and TW2.6/shALDH2 cells were plated on 6 cm plates with complete DMEM/F12 (10% FBS) at a density of $7.5x10^5$ cells/plate for 24 h at 37˚C in 5% CO_2. Subsequently, 0.5 pCMV6-AV-GFP (OriGene; cat. no. #PS100010) and 4.5 μg pGL4.32 (luc2P/NF-κB-RE/Hygro) [Promega Corporation; E8491, NF-κB response element (33-84), 5'-GGGAATTTCCGGGGACTTTCCGGG AATTTCCGGGGACTTTCCGGGAATTTCC-3'] plasmid were co-transfected into cells using TransIT-X2 (Mirus Bio, LLC; cat. no. #MIR 6000). Following 48 h incubation, $1x10^4$ cells with DMEM/F12 (10% FBS) were plated in 96-well plates for 6 h at 37˚C in 5% CO_2 and subsequent analyses. TW2.6/shALDH2 cells were treated with N-acetyl-L-cysteine (NAC, 10 mM; Table SIV) for 12 h at 37˚C in 5% CO_2. A ONE-Glo Luciferase assay kit (Promega Corporation; cat. no. #E6120) and a luminometer (FLUOstar Omega; BMG Labtech GmbH) were used to measure the green fluorescence and luciferase signals. pCMV6-AV-GFP was used as internal control.

H_2O_2 treatment. SAS/ALDH2 cells ($5x10^5$ cells/well) were plated in a 6-well plate and incubated overnight at 37˚C in 5% CO_2. H_2O_2 (80 μM; Table SIV) was added at 37˚C in 5% CO_2 overnight. After 24 h, cells were examined using RT-qPCR to examine *VEGFC* expression.

Colony formation assay. TW2.6/shluc, TW2.6/shALDH2, SAS/Vector, SAS/ALDH2, MTCQ1/Vector, and MTCQ1/ALDH2 HNC cells (4,000 cells/well) were plated in a 6-well plate. After being incubated for 7 days at 37˚C and 5% CO_2, the resulting cell colonies were fixed with 1% formalin for 30 min at room tempature and stained with crystal violet for 30 min at room tempature. ImageJ software (version 1.53t, National Institutes of Health) was used to count the number of colonies (diameter >0.1 cm).

Statistical analysis. Data are shown as the mean ± standard deviation of ≥3 independent repeats. The data analyses used the Student's t- and χ^2 parametric tests, while Mann-Whitney U and Fisher's exact test were employed for non-parametric tests. One-way ANOVA followed by Tukey's post hoc test was used used for multiple group comparisons. Correlation analysis was determined by Spearman's correlation. Prognostic importance of covariates was evaluated through Cox proportional hazards regression in both univariate and multivariate models. Kaplan-Meier method was applied to examine survival curves and the log-rank test was used to compare survival rates between groups. All statistical tests were two-tailed. $P<0.05$ was considered to indicate a statistically significant difference.

Results

ALDH family genes are downregulated in HNC tumor tissue. To identify the metabolic pathways involved in the initiation and progression of HNC, genes with enzyme annotations that showed differential expression in tumor compared with normal tissues from patients with HNC in the GSE6631 dataset were analyzed (Fig. 1A; Table SV). Based on 150 genes that showed differential expression in HNC compared with normal tissue (Table SV), pathways were filtered based on the z-scores with z-score <-2.0 indicating inhibition (Table SVI). IPA revealed that three of the top 15 enriched pathways were 'ethanol degradation II' and 'Ethanol Degradation IV' (Fig. 1B; Table SVI); the remaining 12 pathways predominantly involved enzymes from the ALDH and ADH families. Notably, all of these genes consistently showed significant downregulation, with the commonly downregulated genes being *ADH1B*, *ALDH2*, *ALDH3A2* and *ALDH9A1*. These enzymes were also found to be downregulated in tumor compared with normal tissues in TCGA/HNC cohort (Fig. 1C). Survival analysis using TCGA/HNC cohort identified *ALDH2* as the only gene significantly associated with overall survival (Fig. 1D).

ALDH2 downregulation is associated with poor clinicopathological characteristics and outcomes in HNC. To investigate the differential protein expression of ALDH2 in HNC, the present study analyzed 60 tumor specimens and their paired adjacent normal tissues using IHC. ALDH2 was significantly downregulated in tumor specimens compared with adjacent normal tissue (Fig. 2A and B), To assess the clinical role of ALDH2 expression in HNC, TMA-1 from 106 patients was evaluated. Low ALDH2 expression in HNC tissue was significantly correlated with higher AJCC T classification, advanced overall stage and increased recurrence rates (Table I). Survival analysis using log-rank test revealed that patients with high ALDH2 expression (n=50) had significantly better overall survival (OS) and disease-free survival (DFS) rates than those with low expression (n=56) (Fig. 2C). Univariate analyses identified low ALDH2 expression and high AJCC T and N stage as poor prognostic factors for OS, whereas multivariate analysis showed the no significance of ALDH2 after adjusting for other variables (Fig. 2D; Table SVII). High ALDH2 expression was an independent favorable factor for DFS (Fig. 2D; Table SVIII).

ALDH2 knockdown enhances the migration and invasion abilities of HNC cells. Functional roles of ALDH2 in HNC cell proliferation, migration and invasion were assessed using MTT and Boyden chamber assay. *ALDH2* was most highly expressed in DOK cells, an oral dysplasia cell line (15) and TW2.6 cells, with the lowest expression observed in SAS cells (Fig. S1A). Based on these expression levels, ALDH2 was knocked down in DOK and TW2.6 cells and ALDH2 was overexpressed in SAS cells. As an oral dysplasia cell line derived from a pre-malignant lesion, DOK cells exhibit higher ALDH2 expression levels and lower invasive and migratory ability compared with other HNC cell lines, making them an ideal model for investigating the early stages of HNC progression and ALDH2 tumor-suppressive function (15,16). Following lentivirus-mediated knockdown of ALDH2 via shRNA, western blot and RT-qPCR showed that endogenous ALDH2 was downregulated in DOK and TW2.6 cells (Fig. 3A). ALDH2 knockdown in DOK and TW2.6 cells significantly increased migration and invasion abilities compared with shluc-infected control cells (Fig. 3B). Conversely, overexpression of ALDH2 in SAS cell significantly reduced their ability to invade and

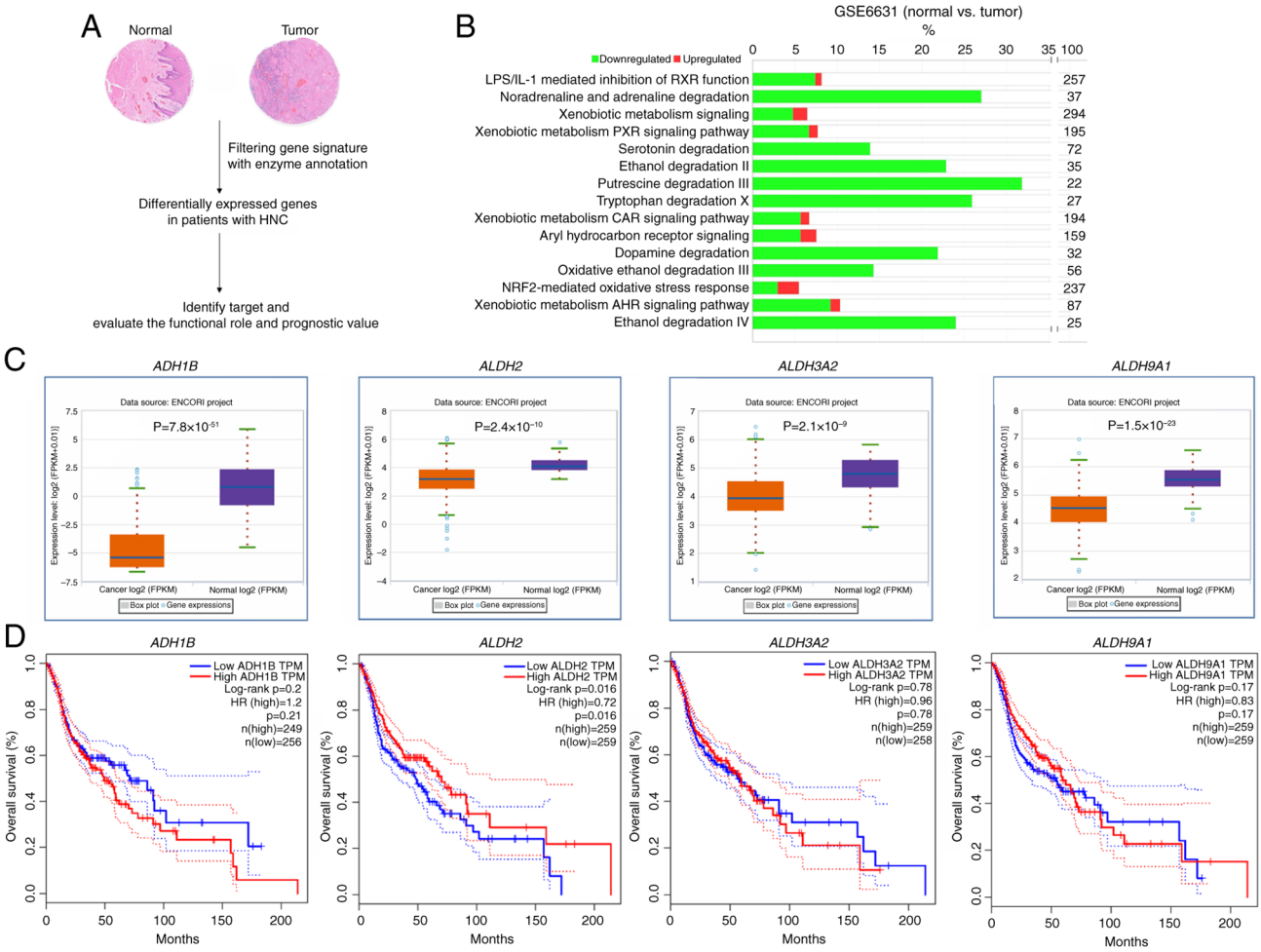

Figure 1. *ALDH* family of genes is downregulated in patients with HNC. (A) Metabolic pathway screening in normal and tumor tissue from patients with HNC. (B) Pathway analysis of differentially expressed genes between normal and tumor tissue in the GSE6631 dataset. (C) mRNA levels of *ADH1B*, *ALDH2*, *ALDH3A2* and *ALDH9A1* in patients (n=502) and healthy samples (n=44), based on data from TCGA database (ENCORI). (D) Overall survival rates from TCGA/HNC cohort as analyzed using GEPIA2 based on expression levels of *ADH1B*, *ALDH2*, *ALDH3A2* and *ALDH9A1*. ALDH, aldehyde dehydrogenase; HNC, Head and Neck Cancer; TCGA, The Cancer Genome Atlas; ADH, alcohol dehydrogenase; FPKM, Fragments Per Kilobase per Million; HR, Hazard Ratio; TPM, Transcripts Per Million.

migrate (Fig. 3C and D). Similarly, colony formation assays showed a significant increase in colony-forming ability in ALDH2-knockdown HNC cells (Fig. 3E). Conversely, ALDH2 overexpression significantly reduced colony formation (Fig. 3F). However, neither overexpression nor knockdown of ALDH2 significantly affected the proliferation of HNC cells (Fig. 3G).

MTCQ1 cells (derived from 4-nitroquinoline 1-oxide-induced tongue carcinoma in C57BL/6 mice) were used to validate the aforementioned results. MTCQ1 cells are characterized by higher invasiveness and clonogenic potential but lower proliferation rate than SAS cells (17). *ALDH2* overexpression in MTCQ1 cells significantly decreased migration, invasion and colony formation without significantly affecting cell proliferation (Fig. S1B-E). These results indicate that ALDH2 influences migration, invasion and colony formation in HNC cells, including DOK cell.

ALDH2 downregulation promotes migration/invasion of HNC cells by activating NF-κB/VEGFC signaling. To elucidate the molecular mechanism mediated by ALDH2, gene expression microarray analysis of ALDH2-knockdown (TW2.6/shALDH2) and control cells (TW2.6/shluc) was performed. ALDH2 knockdown resulted in the upregulation of 980 and the downregulation of 748 genes, with an absolute 2-fold change as the threshold. IPA on these differentially expressed genes, identified tumor necrosis factor (TNF) as the top upstream regulator (Fig. S2A; Table SIX). Pathway analysis showed that 'NF-κB signaling' pathway was significantly upregulated following ALDH2 knockdown, with a z-score of 2.324 (Table SX).

Effect of ALDH2 on NF-κB signaling was assessed in ALDH2-knockdown cells. Knockdown of ALDH2 in TW2.6 cells resulted in increased levels of phosphorylated (p)NF-κB (Fig. 4A). Conversely, ALDH2 overexpression in SAS cells led to a significant decrease in pNF-κB expression (Fig. 4B). Silencing *RELA*) using siRNA markedly inhibited the migration and invasion activity of ALDH2-knockdown cells (Figs. 4B and S2B and C). These results suggested that ALDH2 mediated cell migration and invasion through NF-κB.

Analysis of microarray data from ALDH2-knockdown TW2.6 cells suggests that VEGFC is a key factor in cancer

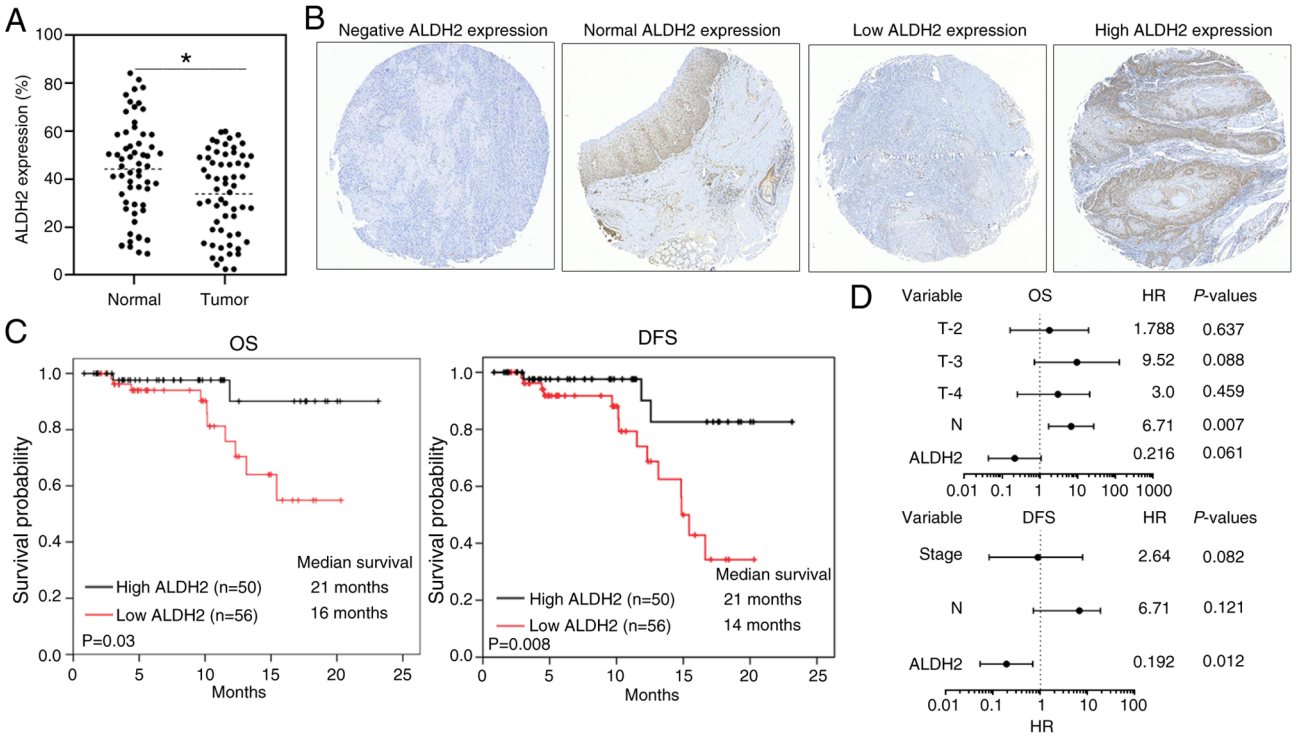

Figure 2. Downregulation of ALDH2 in HNC and its association with survival. (A) Quantification of ALDH2 expression in 60 paired HNC specimens. (B) Representative IHC of ALDH2 expression in HNC tissues (magnification, x10). (C) Kaplan-Meier survival curves illustrating the association between ALDH2 expression and OS and DFS in patients with HNC based on IHC data. (D) Multivariate Cox regression hazard ratio to identify independent risk factors for OS and DFS. *P<0.05. ALDH2, aldehyde dehydrogenase 2; HNC, Head and Neck Cancer; IHC, Immunohistochemistry; OS, Overall Survival; DFS, Disease-Free Survival; HR, Hazard ratio.

progression and is regulated by NF-κB (18). RT-qPCR confirmed that *VEGFC* was significantly upregulated in ALDH2-knockdown cells (Fig. 4D), whereas its expression was notably decreased in ALDH2-overexpressing cells (Figs. 4E and S2D). ALDH2 knockdown enhanced cell migration and invasion, which were significantly suppressed following treatment with a VEGFC-neutralizing antibody (Fig. 4F). To determine whether NF-κB mediates VEGFC expression in ALDH2-knockdown cells, NF-κB inhibitor Bay11-7082 was used, which inhibits IκBα phosphorylation (19). The present results showed a significant decrease in *VEGFC* levels and migration and invasion of TW2.6/shALDH2 cells upon NF-κB inhibition (Fig. 4G and H). These findings confirm that ALDH2 suppression activates the NF-κB/VEGFC axis, leading to aggressiveness of HNC cells.

VEGFC levels are negatively correlated with ALDH2 and positively correlated with poor survival in HNC. ALDH2 and VEGFC expression in HNC tissue was examined via immunohistochemistry in 84 HNC samples from TMA-2. This revealed a negative correlation (Spearman correlation coefficient=-0.173; Fig. 5A), suggesting a potential suppressive effect of ALDH2 on VEGFC. Although VEGFC expression alone did not significantly influence OS (Fig. 5B), the combination of high ALDH2 and low VEGFC levels was associated with greater survival probability compared with the low ALDH2 and high VEGFC (Fig. 5C). In transcriptomic data of 502 patients from TCGA/HNC cohort, there was a consistent inverse relationship between *ALDH2* and *VEGFC* (r=-0.245, Fig. 5D), supporting the protein-level findings. Additionally, GEPIA2 platform showed significantly higher *VEGFC* levels in tumor tissue (n=519) compared with normal (n=44; Fig. 5E). Survival analysis further demonstrated that patients with low *VEGFC* levels (*VEGFC*^{low}, n=248) had improved OS (Fig. 5F). Further analysis of the combined expression levels of *ALDH2* and *VEGFC* revealed that *ALDH2*^{high}/VEGFC^{low} (n=134) had the most favorable survival outcome, whereas patients with *ALDH2*^{low}/*VEGFC*^{high} (n=135) exhibited the poorest prognosis (Fig. 5G).

ALDH2 agonist Alda-1 mitigates acetaldehyde-induced VEGFC expression of HNC cells. Based on enhancement of malignant traits in HNC cells following ALDH2 knockdown, the present study aimed to determine the effect of modulating the enzyme activity of ALDH2 using an antagonist and agonist, particularly focusing on its effects mediated by NF-κB/VEGFC signaling pathway. Daidzin (isoflavone glycoside), a specific ALDH2 antagonist, was used to treat TW2.6 cells. Daidzin resulted in marked increase in pNF-κB expression in TW2.6 cells (Fig. 6A), accompanied by enhanced *VEGFC* levels, however this was not significant (Fig. 6B). In ALDH2-overexpressing SAS cells, daidzin treatment not only increased *VEGFC* levels but also restored the migration and invasion capacities of SAS/ALDH2 cells (Figs. 6C and D and S3A). To investigate the potential of ALDH2 agonist Alda-1 for decreasing cancer aggressiveness, its effect on viability in SAS cells was assessed at various concentrations. Alda-1 treatment showed minimal cytotoxicity in SAS cells, with <25 μM showing no significant decrease in cell viability across the tested range.However, 50 μM of Alda-1 significantly reduced

Table I. Correlation between ALDH2 expression and clinicopathological characteristics in patients with head and neck cancer.

Characteristic	Total (n=106)	Low ALDH2 (n=56)	High ALDH2 (n=50)	P-value
Sex (%)				
Female	15 (14.2)	5 (8.9)	10 (20.0)	0.162
Male	91 (85.8)	51 (91.1)	40 (80.0)	
Age, years (%)				
<60	55 (51.9)	27 (48.2)	28 (56.0)	0.443
≥60	51 (48.1)	29 (51.8)	22 (44.0)	
T stage (%)				
1	40 (37.7)	17 (30.3)	23 (46.0)	0.013
2	29 (27.3)	12 (21.4)	17 (34.0)	
3	6 (5.7)	3 (5.4)	3 (6.0)	
4	31 (29.3)	24 (42.9)	7 (14.0)	
N stage (%)				
0	82 (77.4)	42 (75.0)	40 (80.0)	0.644
+	24 (22.6)	14 (25.0)	10 (20.0)	
Stage (%)				
I/II	57 (53.8)	24 (42.8)	33 (66.0)	0.020
III/IV	49 (46.2)	32 (57.2)	17 (34.0)	
Alcohol consumption (%)				
No	25 (23.6)	10 (17.9)	15 (30.0)	0.172
Yes	81 (76.4)	46 (82.1)	35 (70.0)	
Betel nut consumption (%)				
No	37 (34.9)	18 (32.1)	19 (38.0)	0.458
Yes	69 (65.1)	38 (67.9)	31 (62.0)	
Smoking status (%)				
No	28 (22.6)	11 (16.9)	17 (28.8)	0.135
Yes	96 (77.4)	54 (83.1)	42 (71.2)	
Radiotherapy (%)				
No	64 (60.3)	31 (55.4)	33 (66.0)	0.321
Yes	42 (39.6)	25 (44.6)	17 (34.0)	
Chemotherapy (%)				
No	91 (85.8)	49 (87.5)	42 (84.0)	0.781
Yes	15 (14.2)	7 (12.5)	8 (16.0)	
Recurrence (%)				
No	89 (84.0)	43 (76.7)	46 (92.0)	0.037
Yes	17 (16.0)	13 (23.3)	4 (8.0)	

ALDH2, aldehyde dehydrogenase 2.

cell viability in SAS cells (Fig. S3B). Furthermore, a previous study showed that treatment with 20 μM Alda-1 increased ALDH2-mediated VISTA (V-domain Ig suppressor of T-cell activation) expression in breast cancer cells (20). Based on this evidence, we used a concentration of 20 μM of Alda-1 for subsequent experiments. At this concentration, Alda-1 significantly reduced *VEGFC* levels and markedly decreased the migratory and invasive ability of SAS cells (Figs. 6E and S3C).

Since pharmacological modulation of ALDH2 activity regulated *VEGFC*-mediated HNC migration and invasion similarly to ALDH2 expression modulation, the present study investigated whether these effects were associated with alcohol metabolism. pNF-κB and *VEGFC* expression were significantly upregulated in TW2.6 cells following treatment with acetaldehyde, the primary metabolite of ethanol (21) (Fig. 6F and G). Furthermore, *VEGFC* expression levels in the groups treated with both acetaldehyde and Alda-1 were comparable with those treated with Alda-1 alone (Fig. 6G).

ALDH2 knockdown increases NF-κB activity via ROS production in HNC cells. Acetaldehyde may promote ROS production to enhance oxidative stress (22). NF-κB is a redox-sensitive transcription factor that can be either activated

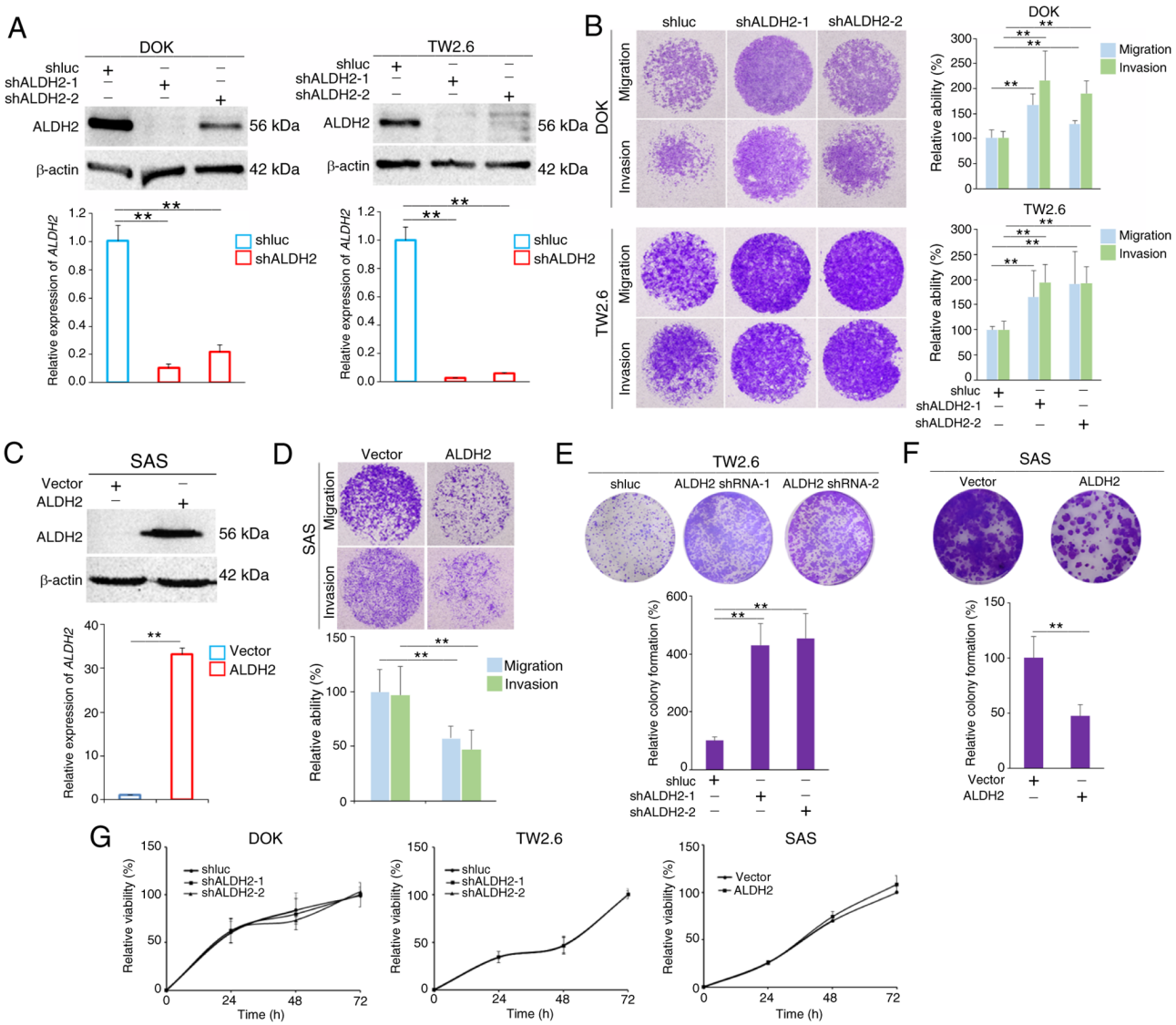

Figure 3. ALDH2 knockdown enhances migration, invasion and colony formation of head and neck cancer cell lines. (A) Western blot and RT-qPCR analysis of ALDH2 expression in DOK and TW2.6 following lentiviral-mediated RNA interference. (B) Effect of ALDH2 knockdown on migration and invasion (16x). (C) Western blot and RT-qPCR analysis of ALDH2 expression following ALDH2 overexpression. (D) Effect of ALDH2 overexpression on migration/invasion capacities of SAS HNC cells (16x). Colony formation assay was performed in (E) TW2.6 and (F) SAS cells (1x). (G) Cell viability. **P<0.01. ALDH, aldehyde dehydrogenase; RT-q, Reverse Transcription-quantitative; sh, short hairpin.

or deactivated by ROS (23). The present study investigated whether ALDH2 regulates NF-κB through ROS modulation. ALDH2 overexpression significantly reduced ROS levels, while ALDH2 knockdown increased ROS levels in HNC cells (Fig. 7A and B). NAC), a free radical scavenger, in ALDH2-knockdown TW2.6 cells significantly suppressed NF-κB activity (Fig. 7C). H_2O_2 led to a marked increase in *VEGFC* levels in ALDH2-overexpressing SAS cells compared with those without H_2O_2 treatment (Fig. 7D). These results collectively suggested that ALDH2 modulates the NF-κB/VEGFC axis by regulating ROS production in HNC cells (Fig. 7E).

Discussion

The present study demonstrated that ALDH2, a common gene with an enzyme signature within the top-ranked altered metabolic pathways in tumor tissue, influences the migration, invasion and colony formation capacities of HNC cells, but not their proliferation. Silencing NF-κB p65 significantly inhibited migration and invasion in *ALDH2*-knockdown cells, with the regulatory mechanism between ALDH2 and NF-κB mediated through its control of ROS production. Treatment of ALDH2-knockdown cells with NF-κB inhibitors or VEGFC-neutralizing antibodies mitigated these enhanced activities by decreasing *VEGFC* expression, confirming that ALDH2-driven migration and invasion are dependent on modulation of the NF-κB/VEGFC axis. *ALDH2*-overexpressing MTCQ1 cells exhibited similar changes in migration, invasion, colony formation and *VEGFC* expression, supporting the present *in vitro* findings. However, the present study lacked *in vivo* validation; animal models are required to determine the effect of ALDH2 on the NF-κB/VEGFC pathway within a complex biological environment. Moreover, the present results suggest that modulating the enzymatic function of ALDH2 induces phenotypical changes similar to those observed

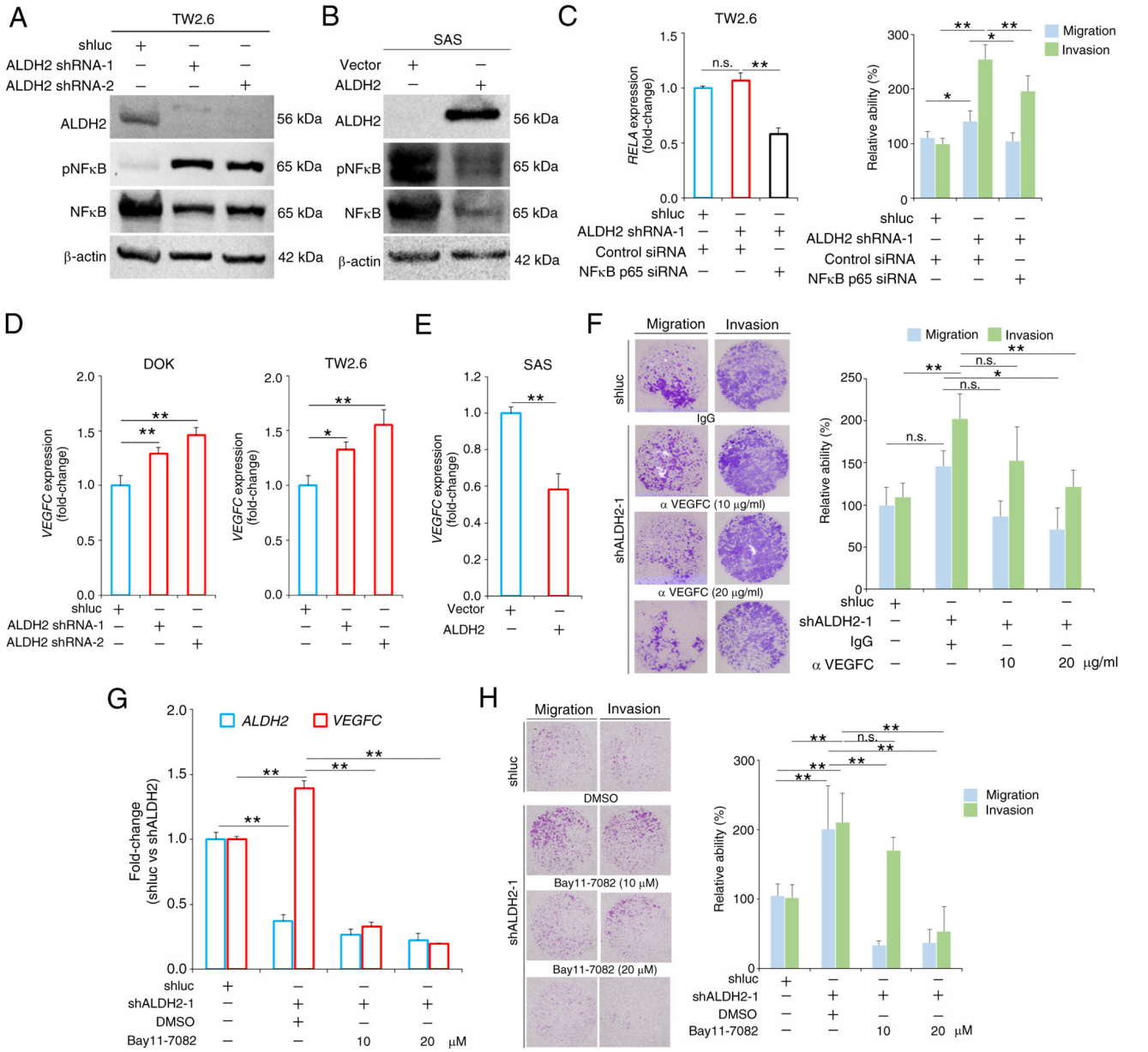

Figure 4. ALDH2 knockdown promotes head and neck cancer cell migration/invasion via VEGFC. (A) Comparative expression levels of ALDH2, pNFκB, and NF-κB in TW2.6 cells. (B) Western blot analysis of ALDH2, pNF-κB, and NF-κB in SAS/ALDH2 cells. (C) RT-qPCR analysis of *RELA* expression and migration and invasion of TW2.6/shALDH2 cells following *RELA* silencing. RT-qPCR analysis of *VEGFC* expression in (D) DOK and TW2.6 cells following ALDH2 knockdown and (E) ALDH2-overexpressing SAS cells. (F) Migration and invasion capabilities of TW2.6/shALDH2 cells following pretreatment with a VEGFC-neutralizing antibody for 30 min. (G) RT-qPCR analysis of *ALDH2* and *VEGFC* expression and (H) migration and invasion of TW2.6/shALDH2 cells after treatment with the NF-κB inhibitor Bay11-7082 (16x). *P<0.05, **P<0.01. n.s., not significant; ALDH, aldehyde dehydrogenase; VEGFC, Vascular Endothelial Growth Factor C; p, phosphorylated; RT-q, Reverse Transcription-quantitative; RELA, NF-κB p65; sh, short hairpin; si, small interfering.

when altering ALDH2 expression levels, through established signaling pathways, even in HNC cells overexpressing ALDH2. Modulating ALDH2 activity with Alda-1 mitigated the acetaldehyde-induced enhancement of the NF-κB/VEGFC axis, consistent with the present IPA findings on altered alcohol metabolism. The inverse association between ALDH2 and VEGFC and the detrimental impact of their combined expression on patient outcomes, positions ALDH2 as a potential metabolic target for HNC treatment, offering novel avenues for therapeutic intervention. Additionally, previous data revealed lower ALDH2 expression in cancer tissues and showed that ALDH2 knockdown increased the half-maximal inhibitory concentration of 5-fluorouracil in HNC cells (24), further emphasizing the role of the metabolic gene *ALDH2* in the characteristic behavior of HNC.

ALDH2 is a key mitochondrial enzyme that forms tetramers and serves a pivotal role in detoxification of acetaldehyde and endogenous aldehydes. Defective ALDH2 enzymes lead to the accumulation of acetaldehyde, inducing DNA damage through formation of DNA adducts and causing genetic and epigenetic instability by forming DNA-protein crosslinks and histone adducts (6-8). Exposure to ethanol-derived acetaldehyde causes chromosomal rearrangements and genomic instability in hematopoietic stem cells, potentially initiating malignancy despite recombination repair activation and p53 deletion (25). Additionally, acetaldehyde-induced DNA

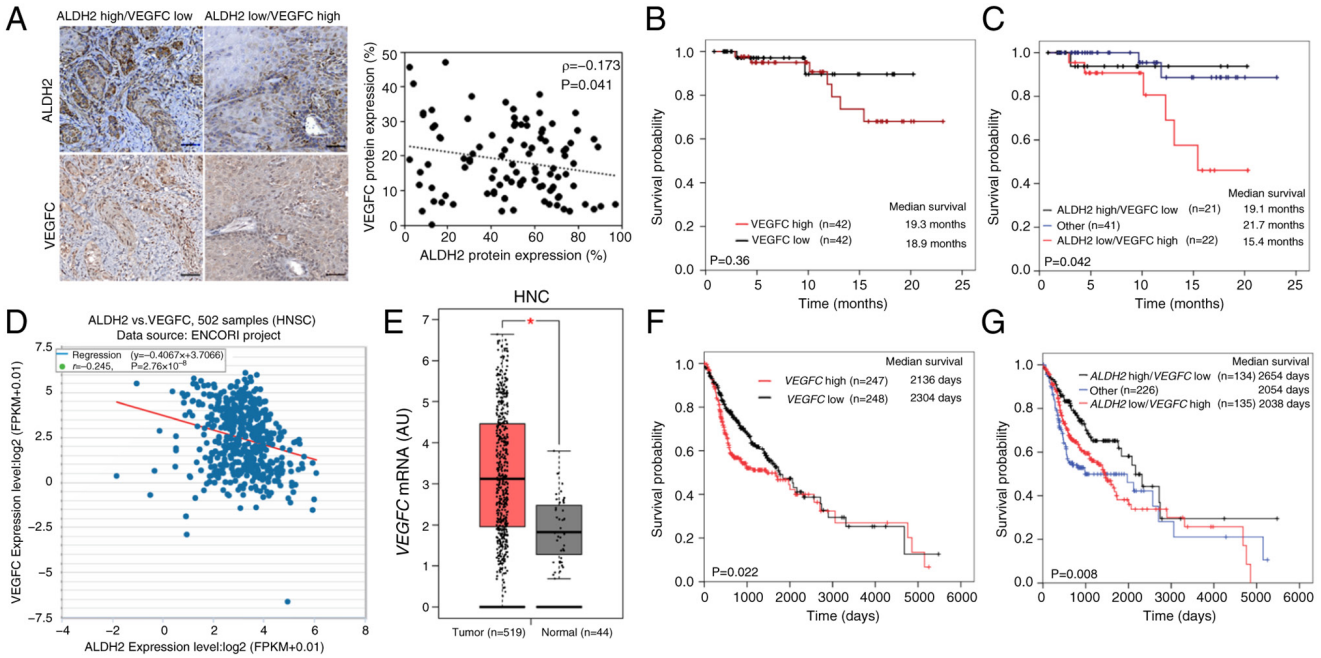

Figure 5. ALDH2 expression is negatively correlated with VEGFC expression in HNC tissues. (A) Representative immunohistochemistry staining and correlation between ALDH2 and VEGFC in HNC tissues.Scale bar: 100 μm. Overall survival analysis according to (B) VEGFC and (C) ALDH2/VEGFC expression in patients with HNC (n=84). (D) Correlation analysis between *ALDH2* and *VEGFC* levels in HNC tissue (ENCORI). (E) Comparison of *VEGFC* mRNA levels in normal (n=44) and tumor tissues (n=519) from The Cancer Genome Atlas/HNC cohort (GEPIA2). *P<0.05. Overall survival analysis according to (F) *VEGFC* and (G) *ALDH2*/*VEGFC* expression in patients with HNC (n=495; OncoLnc). Other, $ALDH2^{low}/VEGFC^{low}$ and $ALDH2^{high}/VEGFC^{high}$ expression; ALDH, aldehyde dehydrogenase; VEGFC, Vascular Endothelial Growth Factor C; HNC, Head and Neck Cancer; AU, arbitrary units; FPKM, Fragments Per Kilobase per Million.

damage, as indicated by γH2AX levels, is decreased in *ALDH2*-overexpressing A549 cells after acetaldehyde exposure, suggesting that ALDH2 suppression leads to acetaldehyde accumulation, which increases DNA damage and enhances the migratory ability of these cells (26). Acetaldehyde further amplifies oxidative stress by producing ROS, similar to the effects of endogenous aldehydes such as 4-HNE, which are generated during redox stress-induced lipid peroxidation (6,7). The cycle of mutual amplification between toxic reactive aldehydes and ROS may exacerbate lipid peroxidation (6,7), highlighting the key role of ALDH2 in maintaining redox homeostasis. Therefore, when cellular antioxidant defenses and energetic adaptability are insufficient to mitigate damage caused by either oxidative stress or aldehydic products, cells may incur mutations in oncogenes or tumor suppressor genes that induce carcinogenesis (27). Western blot analysis revealed background bands in the 45-60 kDa range in ALDH2 knockdown HNC cells. Similar background bands have also been reported in a previous study on lung cancer (26), which may be attributed to the presence of two ALDH2 isoforms at the protein level, with molecular weights of 56 and 46 kDa (28). However, specific roles of ALDH2 isoforms in HNC remain unclear and warrant further investigation.

As TNF modulates NF-κB signaling (29,30), knockdown of ALDH2 activated TNF signal, these findings highlight its potential involvement in ALDH2-mediated pathways. The impact of aldehydic products on NF-κB has been established (31,32). Acetaldehyde activates NF-κB in HepG2 cells via IκBα degradation and protein kinase C signaling (31). By contrast, 4-HNE may inhibit the NF-κB pathway and inactivate Bcl-2 via IKK-mediated phosphorylation, suggesting NF-κB functions as an anti-apoptotic element (32). ROS can either activate or suppress NF-κB, depending on cellular context. This dual role of ROS is complex, as ROS can activate NF-κB by promoting alternative phosphorylation of IκBα or enhancing IKK activity via NF-κB essential modulator (NEMO) dimerization (23). Conversely, ROS may inhibit NF-κB by oxidizing key cysteine residues in its subunits, which decreases the ability of NF-κB to bind to DNA (23). A previous study demonstrated that elevated ROS levels from increased mitochondrial fission may activate NF-κB via NF-κB inhibitor alpha (NFKBIA) and IKK, promoting liver cancer cell survival (33). The present findings demonstrated that, in HNC, ROS enhanced NF-κB activity, which served a key role in activating VEGFC. This regulation underscores the involvement of ROS in promoting HNC progression. However, further mechanistic studies are warrated to elucidate redox-sensitive sites within the NF-κB that respond to ROS changes induced by ALDH2.

The present study identified ALDH2 as a tumor suppressor in HNC, similar to its roles in lung and liver cancer (26,34,35). The present data highlight the metabolic role of ALDH2 in modulating cancer cell phenotypes, as Alda-1 administration reversed acetaldehyde-induced *VEGFC* expression. This confirms that the pharmacological modulation of ALDH2 significantly impacts HNC cell behavior regardless of ALDH2 expression levels. Alda-1, a selective activator of ALDH2, enhances ALDH2 activity by functioning as a structural chaperone (36) and protects ALDH2 from aldehyde-induced inactivation by preventing access to key cysteine residues (37). Preclinical *in vivo* studies have shown promising results regarding the efficacy and safety of Alda-1 in oxidative

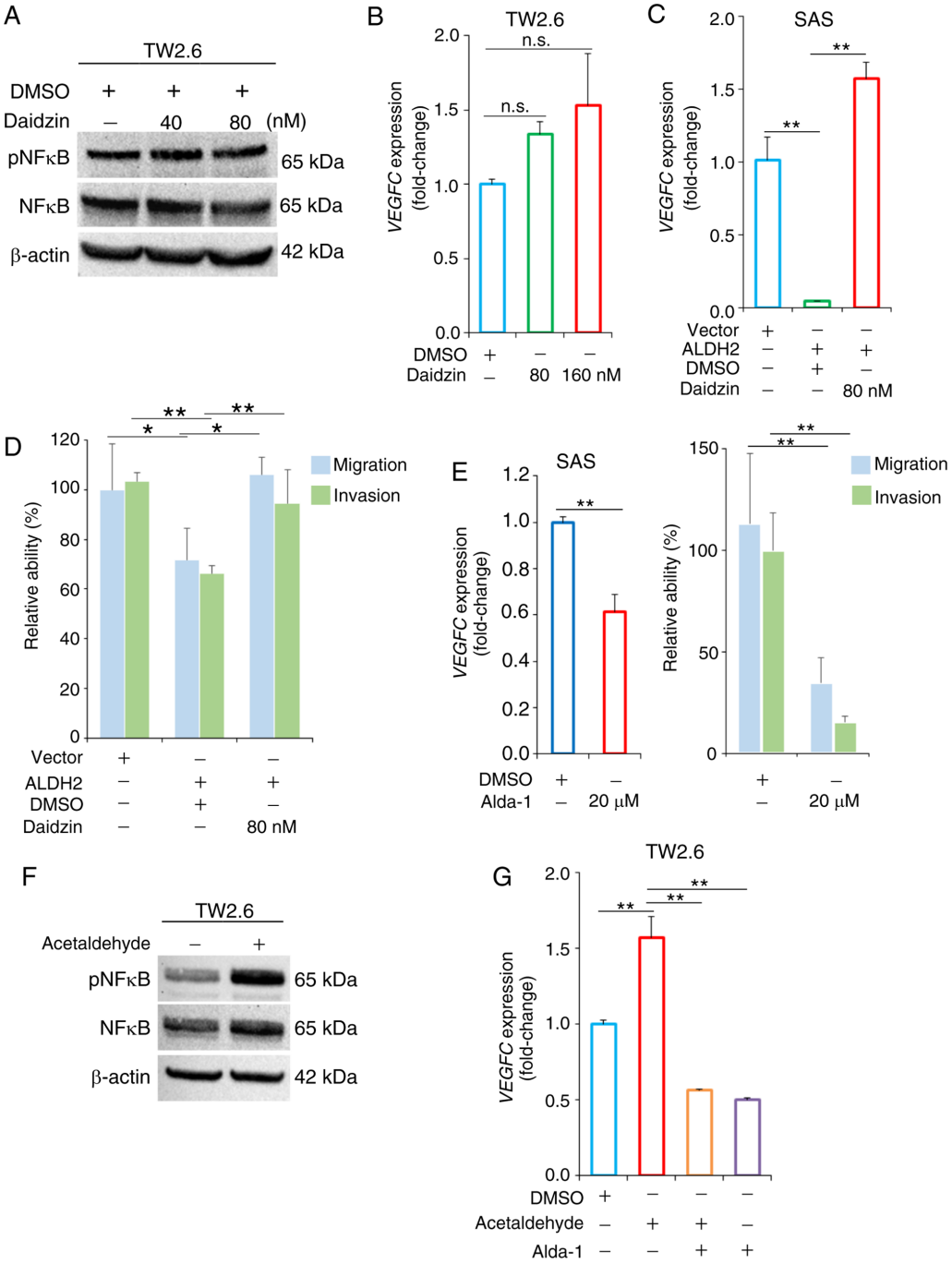

Figure 6. ALDH2 agonist Alda-1 decreases the malignant characteristics of head and neck cancer cells. (A) TW2.6 cells were treated with DMSO or Daidzin for 48 h and levels of pNF-κB and NF-κB were analyzed through western blotting. RT-qPCR analysis of *VEGFC* levels in (B) TW2.6 cells and (C) SAS/ALDH2 and (D) migration and invasion of SAS/ALDH2 cells following Daidzin treatment. (E) RT-qPCR analysis of *VEGFC* levels and migration and invasion capabilities of SAS cells after Alda-1 (20 μM) treatment. (F) Western blotting was used to assess levels of pNF-κB and NF-κB in TW2.6 cells after treatment with acetaldehyde (10 μM) for 1 h. (G) Effect of acetaldehyde (10 μM) alone or combined with Alda-1 (20 μM) in TW2.6 cells. *VEGFC* levels were measured by RT-qPCR. *P<0.05, **P<0.01. ALDH, aldehyde dehydrogenase; p, ; RT-q, reverse transcription-quantitative; n.s., not significant; VEGFC, Vascular Endothelial Growth Factor C.

stress-related disorders affecting the brain, heart, lung, liver and retina (6,7,38). The underlying mechanism primarily involves reducing ROS and aldehyde-mediated signaling pathways (6,7,38). In esophageal cancer, previous *in vivo* findings have demonstrated that Alda-1 reduces alcohol-induced esophageal DNA damage in genetically modified mice with *ALDH2* polymorphisms (39) and inhibits the expansion of CD44-high cancer stem cells, which are associated with tumor initiation and chemoresistance (40). The present investigation confirmed that ALDH2 is a prognostic factor with significant correlations to T classification and overall stage in human HNC tissue. The activation of ALDH2 by Alda-1 inhibited the malignant features of HNC cells through the NF-κB/VEGFC axis. Overall, these findings suggested that Alda-1 is a viable therapeutic strategy for HNC. However, further studies are warranted to clarify the specific dose-effect association,

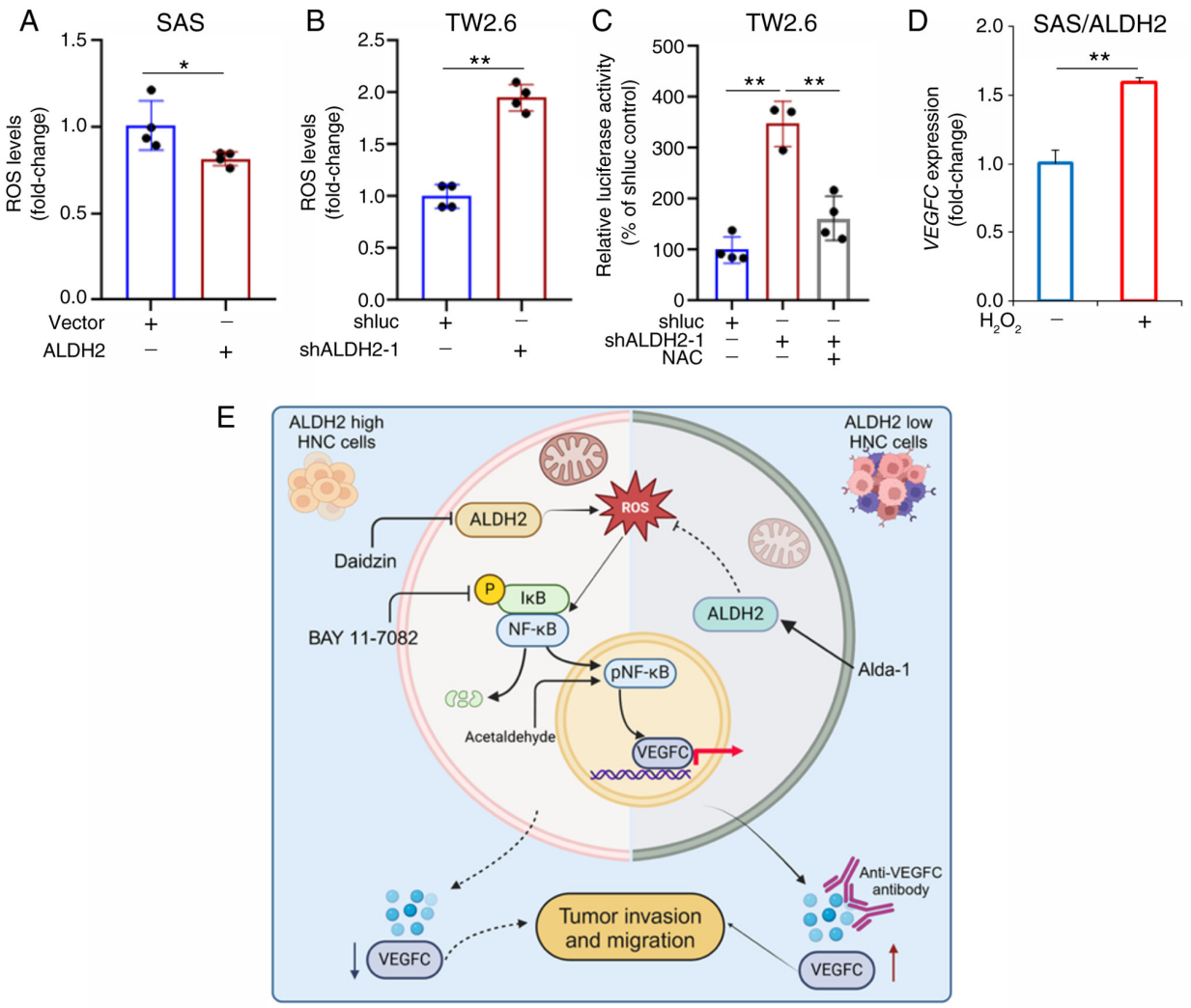

Figure 7. ALDH2 inhibits ROS production in HNC cells. ROS levels in (A) SAS and (B) TW2.6 cells. (C) Reporter assay for NF-κB activity in TW2.6 cells. (D) Reverse transcription-quantitative PCR analysis of *VEGFC* expression in SAS/ALDH2 cells treated with H_2O_2 for 24 h. (E) ALDH2 inhibits the NF-κB signaling pathway, leading to the downregulation of VEGFC expression in HNC cells. *P<0.05, **P<0.01. ALDH, aldehyde dehydrogenase; ROS, reactive oxygen species; HNC, Head and Neck Cancer; VEGFC, Vascular Endothelial Growth Factor C; p, P-value.

potential side effects and clinical feasibility of Alda-1 to support its application as a therapeutic agent for HNC.

VEGFC, a member of the VEGF/platelet-derived growth factor family, contains conserved NF-κB binding sites in its promoter, indicating regulation via the NF-κB pathway (41). Once processed into its mature form, VEGFC binds to VEGFR-3 and neuropilin-2 (NRP2) on lymphatic endothelial cells to facilitate lymphatic metastasis (42,43). VEGFC signaling is crucial for establishing premetastatic niches in sentinel lymph nodes (44,45), facilitating spread, colonization and maintenance of disseminated tumor cells (46-48). In HNC, elevated VEGFC expression is associated with larger tumor size, higher recurrence rate and poorer survival outcome (49-51) than low expression, highlighting its significance as a therapeutic target. Current VEGF-targeted therapies that use tyrosine kinases against VEGFR have shown promise in clinical trials for metastatic HNC (52-54). For example, a phase II trial of axitinib reported a disease control rate of 76.7% and median OS of 10.9 months (55). However, evidence supporting the effectiveness of anti-VEGFC monoclonal antibodies in this context is lacking. While studiy in clear cell renal cell carcinoma suggests benefits in targeting VEGFC (53), especially in cells overexpressing VEGFR-3 and NRP2, resistance to anti-angiogenic therapy can develop through the upregulation of hypoxia-inducible factor-1α, angiopoietin-2 and basic fibroblast growth factor (56). Thus, addressing resistance to anti-VEGFC treatment may require targeting upstream regulatory molecules simultaneously. The present findings indicate that ALDH2 regulated VEGFC by modulating NF-κB activity, further highlighting the potential of pharmacologically enhancing ALDH2 function to combat metastatic HNC.

Taken together, the present findings confirmed that ALDH2 served a critical role in regulating alcohol metabolism in HNC, with its downregulation linked to poor survival outcome. Alda-1 restored ALDH2 activity, effectively inhibiting acetaldehyde-induced upregulation of NF-κB/VEGFC axis and inhibiting migration and invasion in HNC. While *in vivo* validation is warranted to confirm these effects, the present results highlight the therapeutic potential of targeting alcohol metabolism via ALDH2 modulation to improve treatment outcome in HNC.

Acknowledgements

The authors would like to thank Professor Michael Hsiao from Academia Sinica, Taipei, Taiwan for kindly providing HNC cell lines.

Funding

The present study was supported by Kaohsiung Veterans General Hospital, Taiwan (grant nos. KSVGH111-098, KSVGH112-094 and KSVGH-113-062), Yen Tjing Ling Medical Foundation (grant no. CI-112-5) and National Science and Technology Council, Taiwan (grant nos. MOST-110-2314-B-075B-014, NSTC-113-2314-B-075B-001, MOST-110-2314-B-075B-009-MY3 and NSTC-113-2314-B-075B-002).

Availability of data and materials

The data generated in the present study may be found in the Gene Expression Omnibus under accession number (GSE253622) or at the following URL: ncbi.nlm.nih.gov/geo/query/acc.cgi?acc=GSE253622.

Authors' contributions

YHL and YFY interpreted data and wrote the manuscript. YHL and JBL performed histopathology experiments. YCL, PLY and CYC performed experiments. YHL and YFY confirm the authenticity of all the raw data. All authors have read and approved the final manuscript.

Ethics approval and consent to participate

The Kaohsiung Veterans General Hospital ethics committee approved the study (approval no. KSVGH23-CT8-10) and waived the requirement for informed consent.

Patient consent for publication

Not applicable.

Competing interests

The authors declare that they have no competing interests.

References

1. Sung H, Ferlay J, Siegel RL, Laversanne M, Soerjomataram I, Jemal A and Bray F: Global cancer statistics 2020: GLOBOCAN estimates of incidence and mortality worldwide for 36 cancers in 185 countries. CA Cancer J Clin 71: 209-249, 2021.
2. Johnson DE, Burtness B, Leemans CR, Lui VWY, Bauman JE and Grandis JR: Head and neck squamous cell carcinoma. Nat Rev Dis Primers 6: 92, 2020.
3. Cancer Genome Atlas Network: Comprehensive genomic characterization of head and neck squamous cell carcinomas. Nature 517: 576-582, 2015.
4. Faubert B, Solmonson A and DeBerardinis RJ: Metabolic reprogramming and cancer progression. Science 368: eaaw5473, 2020.
5. Xia L, Oyang L, Lin J, Tan S, Han Y, Wu N, Yi P, Tang L, Pan Q, Rao S, *et al*: The cancer metabolic reprogramming and immune response. Mol Cancer 20: 28, 2021.
6. Chen CH, Ferreira JC, Gross ER and Mochly-Rosen D: Targeting aldehyde dehydrogenase 2: New therapeutic opportunities. Physiol Rev 94: 1-34, 2014.
7. Gao J, Hao Y, Piao X and Gu X: Aldehyde dehydrogenase 2 as a therapeutic target in oxidative stress-related diseases: Post-translational modifications deserve more attention. Int J Mol Sci 23: 2682, 2022.
8. Chen D, Fang L, Li H and Jin C: The effects of acetaldehyde exposure on histone modifications and chromatin structure in human lung bronchial epithelial cells. Environ Mol Mutagen 59: 375-385, 2018.
9. Lee WT, Hsiao JR, Ou CY, Huang CC, Chang CC, Tsai ST, Chen KC, Huang JS, Wong TY, Lai YH, *et al*: The influence of prediagnosis alcohol consumption and the polymorphisms of ethanol-metabolizing genes on the survival of head and neck cancer patients. Cancer Epidemiol Biomarkers Prev 28: 248-257, 2019.
10. Tang Z, Li C, Kang B, Gao G, Li C and Zhang Z: GEPIA: A web server for cancer and normal gene expression profiling and interactive analyses. Nucleic Acids Res 45 (W1): W98-W102, 2017.
11. Edge SB and Compton CC: The American joint committee on cancer: The 7th edition of the AJCC cancer staging manual and the future of TNM. Ann Surg Oncol 17: 1471-1474, 2010.
12. Tseng HH, Tseng YK, You JJ, Kang BH, Wang TH, Yang CM, Chen HC, Liou HH, Liu PF, Ger LP and Tsai KW: Next-generation sequencing for microRNA profiling: MicroRNA-21-3p promotes oral cancer metastasis. Anticancer Res 37: 1059-1066, 2017.
13. Liu CW, Hua KT, Li KC, Kao HF, Hong RL, Ko JY, Hsiao M, Kuo ML and Tan CT: Histone Methyltransferase G9a drives chemotherapy resistance by regulating the glutamate-cysteine ligase catalytic subunit in head and neck squamous cell carcinoma. Mol Cancer Ther 16: 1421-1434, 2017.
14. Livak KJ and Schmittgen TD: Analysis of relative gene expression data using real-time quantitative PCR and the 2(-Delta Delta C(T)) method. Methods 25: 402-408, 2001.
15. Chang SE, Foster S, Betts D and Marnock WE: DOK, a cell line established from human dysplastic oral mucosa, shows a partially transformed non-malignant phenotype. Int J Cancer 52: 896-902, 1992.
16. Bs A, P A, As SG, A P and J VP: Analysis of differentially expressed genes in dysplastic oral keratinocyte cell line and their role in the development of HNSCC. J Stomatol Oral Maxillofac Surg 125: 101928, 2024.
17. Chen YF, Chang KW, Yang IT, Tu HF and Lin SC: Establishment of syngeneic murine model for oral cancer therapy. Oral Oncol 95: 194-201, 2019.
18. Lin C, Song L, Gong H, Liu A, Lin X, Wu J, Li M and Li J: Editor's Note: Nkx2-8 downregulation promotes angiogenesis and activates NF-κB in esophageal cancer. Cancer Res 82: 1670, 2022.
19. Strickson S, Campbell DG, Emmerich CH, Knebel A, Plater L, Ritorto MS, Shpiro N and Cohen P: The anti-inflammatory drug BAY 11-7082 suppresses the MyD88-dependent signalling network by targeting the ubiquitin system. Biochem J 451: 427-437, 2013.
20. Chen Y, Sun J, Liu J, Wei Y, Wang X, Fang H, Du H, Huang J, Li Q, Ren G, *et al*: Aldehyde dehydrogenase 2-mediated aldehyde metabolism promotes tumor immune evasion by regulating the NOD/VISTA axis. J Immunother Cancer 11: e007487, 2023.
21. Lachenmeier DW and Sohnius EM: The role of acetaldehyde outside ethanol metabolism in the carcinogenicity of alcoholic beverages: Evidence from a large chemical survey. Food Chem Toxicol 46: 2903-2911, 2008.
22. Li SY, Gomelsky M, Duan J, Zhang Z, Gomelsky L, Zhang X, Epstein PN and Ren J: Overexpression of aldehyde dehydrogenase-2 (ALDH2) transgene prevents acetaldehyde-induced cell injury in human umbilical vein endothelial cells: Role of ERK and p38 mitogen-activated protein kinase. J Biol Chem 279: 11244-11252, 2004.
23. Morgan MJ and Liu ZG: Crosstalk of reactive oxygen species and NF-kappaB signaling. Cell Res 21: 103-115, 2011.
24. Lin YH, Yang YF, Liao JB, Chang TS, Janesha UGS and Shiue YL: Analysis of aldehyde dehydrogenase 2 as a prognostic marker associated with immune cell infiltration and chemotherapy efficacy in head and neck squamous cell carcinoma. J Cancer 14: 1689-1706, 2023.
25. Garaycoechea JI, Crossan GP, Langevin F, Mulderrig L, Louzada S, Yang F, Guilbaud G, Park N, Roerink S, Nik-Zainal S, *et al*: Alcohol and endogenous aldehydes damage chromosomes and mutate stem cells. Nature 553: 171-177, 2018.

26. Li K, Guo W, Li Z, Wang Y, Sun B, Xu D, Ling J, Song H, Liao Y, Wang T, *et al*: ALDH2 repression promotes lung tumor progression via accumulated acetaldehyde and DNA damage. Neoplasia 21: 602-614, 2019.
27. Dalleau S, Baradat M, Guéraud F and Huc L: Cell death and diseases related to oxidative stress: 4-Hydroxynonenal (HNE) in the balance. Cell Death Differ 20: 1615-1630, 2013.
28. Zahn-Zabal M, Michel PA, Gateau A, Nikitin F, Schaeffer M, Audot E, Gaudet P, Duek PD, Teixeira D, Rech de Laval V, *et al*: The neXtProt knowledgebase in 2020: Data, tools and usability improvements. Nucleic Acids Res 48 (D1): D328-D334, 2020.
29. Legler DF, Micheau O, Doucey MA, Tschopp J and Bron C: Recruitment of TNF receptor 1 to lipid rafts is essential for TNFalpha-mediated NF-kappaB activation. Immunity 18: 655-664, 2003.
30. Yang YF, Jan YH, Liu YP, Yang CJ, Su CY, Chang YC, Lai TC, Chiou J, Tsai HY, Lu J, *et al*: Squalene synthase induces tumor necrosis factor receptor 1 enrichment in lipid rafts to promote lung cancer metastasis. Am J Respir Crit Care Med 190: 675-687, 2014.
31. Román J, Giménez A, Lluis JM, Gassó M, Rubio M, Caballeria J, Parés A, Rodés J and Fernández-Checa JC: Enhanced DNA binding and activation of transcription factors NF-kappa B and AP-1 by acetaldehyde in HEPG2 cells. J Biol Chem 275: 14684-14690, 2000.
32. Timucin AC and Basaga H: Pro-apoptotic effects of lipid oxidation products: HNE at the crossroads of NF-κB pathway and anti-apoptotic Bcl-2. Free Radic Biol Med 111: 209-218, 2017.
33. Huang Q, Zhan L, Cao H, Li J, Lyu Y, Guo X, Zhang J, Ji L, Ren T, An J, *et al*: Increased mitochondrial fission promotes autophagy and hepatocellular carcinoma cell survival through the ROS-modulated coordinated regulation of the NFKB and TP53 pathways. Autophagy 12: 999-1014, 2016.
34. Chen X, Legrand AJ, Cunniffe S, Hume S, Poletto M, Vaz B, Ramadan K, Yao D and Dianov GL: Interplay between base excision repair protein XRCC1 and ALDH2 predicts overall survival in lung and liver cancer patients. Cell Oncol (Dordr) 41: 527-539, 2018.
35. Seo W, Gao Y, He Y, Sun J, Xu H, Feng D, Park SH, Cho YE, Guillot A, Ren T, *et al*: ALDH2 deficiency promotes alcohol-associated liver cancer by activating oncogenic pathways via oxidized DNA-enriched extracellular vesicles. J Hepatol 71: 1000-1011, 2019.
36. Perez-Miller S, Younus H, Vanam R, Chen CH, Mochly-Rosen D and Hurley TD: Alda-1 is an agonist and chemical chaperone for the common human aldehyde dehydrogenase 2 variant. Nat Struct Mol Biol 17: 159-164, 2010.
37. Chen CH, Budas GR, Churchill EN, Disatnik MH, Hurley TD and Mochly-Rosen D: Activation of aldehyde dehydrogenase-2 reduces ischemic damage to the heart. Science 321: 1493-1495, 2008.
38. Kimura M, Yokoyama A and Higuchi S: Aldehyde dehydrogenase-2 as a therapeutic target. Expert Opin Ther Targets 23: 955-966, 2019.
39. Hirohashi K, Ohashi S, Amanuma Y, Nakai Y, Ida T, Baba K, Mitani Y, Mizumoto A, Yamamoto Y, Kikuchi O, *et al*: Protective effects of Alda-1, an ALDH2 activator, on alcohol-derived DNA damage in the esophagus of human ALDH2*2 (Glu504Lys) knock-in mice. Carcinogenesis 41: 194-202, 2020.
40. Flashner S, Shimonosono M, Tomita Y, Matsuura N, Ohashi S, Muto M, Klein-Szanto AJ, Alan Diehl J, Chen CH, Mochly-Rosen D, *et al*: ALDH2 dysfunction and alcohol cooperate in cancer stem cell enrichment. Carcinogenesis 45: 95-106, 2024.
41. Chilov D, Kukk E, Taira S, Jeltsch M, Kaukonen J, Palotie A, Joukov V and Alitalo K: Genomic organization of human and mouse genes for vascular endothelial growth factor C. J Biol Chem 272: 25176-25183, 1997.
42. Wang J, Huang Y, Zhang J, Wei Y, Mahoud S, Bakheet AM, Wang L, Zhou S and Tang J: Pathway-related molecules of VEGFC/D-VEGFR3/NRP2 axis in tumor lymphangiogenesis and lymphatic metastasis. Clin Chim Acta 461: 165-171, 2016.
43. Wang J, Huang Y, Zhang J, Xing B, Xuan W, Wang H, Huang H, Yang Jand Tang J: NRP-2 in tumor lymphangiogenesis and lymphatic metastasis. Cancer Lett 418: 176-184, 2018.
44. Liersch R, Hirakawa S, Berdel WE, Mesters RM and Detmar M: Induced lymphatic sinus hyperplasia in sentinel lymph nodes by VEGF-C as the earliest premetastatic indicator. Int J Oncol 41: 2073-2078, 2012.
45. Hirakawa S, Brown LF, Kodama S, Paavonen K, Alitalo K and Detmar M: VEGF-C-induced lymphangiogenesis in sentinel lymph nodes promotes tumor metastasis to distant sites. Blood 109: 1010-1017, 2007.
46. Karaman S and Detmar M: Mechanisms of lymphatic metastasis. J Clin Invest 124: 922-928, 2014.
47. Kong D, Zhou H, Neelakantan D, Hughes CJ, Hsu JY, Srinivasan RR, Lewis MT and Ford HL: VEGF-C mediates tumor growth and metastasis through promoting EMT-epithelial breast cancer cell crosstalk. Oncogene 40: 964-979, 2021.
48. Banerjee K, Kerzel T, Bekkhus T, de Souza Ferreira S, Wallmann T, Wallerius M, Landwehr LS, Agardy DA, Schauer N, Malmerfeldt A, *et al*: VEGF-C-expressing TAMs rewire the metastatic fate of breast cancer cells. Cell Rep 42: 113507, 2023.
49. Neuchrist C, Erovic BM, Handisurya A, Fischer MB, Steiner GE, Hollemann D, Gedlicka C, Saaristo A and Burian M: Vascular endothelial growth factor C and vascular endothelial growth factor receptor 3 expression in squamous cell carcinomas of the head and neck. Head Neck 25: 464-474, 2003.
50. Fei J, Hong A, Dobbins TA, Jones D, Lee CS, Loo C, Al-Ghamdi M, Harnett GB, Clark J, O'Brien CJ and Rose B: Prognostic significance of vascular endothelial growth factor in squamous cell carcinomas of the tonsil in relation to human papillomavirus status and epidermal growth factor receptor. Ann Surg Oncol 16: 2908-2917, 2009.
51. Siemert J, Wald T, Kolb M, Pettinella I, Böhm U, Pirlich M, Wiegand S, Dietz A and Wichmann G: Pre-therapeutic VEGF level in plasma is a prognostic bio-marker in head and neck squamous cell carcinoma (HNSCC). Cancers (Basel) 13: 3781, 2021.
52. Limaye S, Riley S, Zhao S, O'Neill A, Posner M, Adkins D, Jaffa Z, Clark J and Haddad R: A randomized phase II study of docetaxel with or without vandetanib in recurrent or metastatic squamous cell carcinoma of head and neck (SCCHN). Oral Oncol 49: 835-841, 2013.
53. Swiecicki PL, Zhao L, Belile E, Sacco AG, Chepeha DB, Dobrosotskaya I, Spector M, Shuman A, Malloy K, Moyer J, *et al*: A phase II study evaluating axitinib in patients with unresectable, recurrent or metastatic head and neck cancer. Invest New Drugs 33: 1248-1256, 2015.
54. Adkins D, Mehan P, Ley J, Siegel MJ, Siegel BA, Dehdashti F, Jiang X, Salama NN, Trinkaus K and Oppelt P: Pazopanib plus cetuximab in recurrent or metastatic head and neck squamous cell carcinoma: An open-label, phase 1b and expansion study. Lancet Oncol 19: 1082-1093, 2018.
55. Dumond A, Montemagno C, Vial V, Grépin R and Pagès G: Anti-vascular endothelial growth factor C antibodies efficiently inhibit the growth of experimental clear cell renal cell carcinomas. Cells 10: 1222, 2021.
56. Ansari MJ, Bokov D, Markov A, Jalil AT, Shalaby MN, Suksatan W, Chupradit S, Al-Ghamdi HS, Shomali N, Zamani A, *et al*: Cancer combination therapies by angiogenesis inhibitors; a comprehensive review. Cell Commun Signal 20: 49, 2022.